WARSAW UNIVERSITY OF TECHNOLOGY Index 351733
FACULTY OF CIVIL ENGINEERING
COMMITTEE FOR CIVIL AND WATER ENGINEERING
POLISH ACADEMY OF SCIENCES ISSN 1230-2945
DOI: 10.24425/ace.2026.158601
ARCHIVES OF CIVIL ENGINEERING
Vol. LXXII ISSUE 2 2026
pp. 155 –168

Research paper

Study on the close distance perforation capabilities of explosively formed penetrators

Sebastian Stanisławek[1], Grzegorz Sławiński[2], Andrzej Morka[3]

Abstract: The paper presents a study of the perforation capabilities of Explosively Formed Penetrators (EFP) at small distances between the charge placement and a target for the selected charge configurations. The specific design of the warhead is considered, where the casing is made of light, low-strength material and the warhead may be installed directly on the obstacle, which makes it valuable for special applications. The problem was solved using modelling and simulation methods, in particular, CFD-FEM implemented in the Ls-Dyna code. It was assumed as an axisymmetric issue in computational fluid dynamics, where space discretization for each option was built with two-dimensional elements, which ensured efficient calculations. The core numerical model was successfully validated based on the available data in quantitative terms. Analyses showed that at close ranges, under two diameters of the liner, the projectile fails to reach its optimal parameters, impacting the target with relatively low velocity. This effectiveness is also deteriorated by the projectile's geometry, which at this moment is still not final. Studies on the projectile's post-perforation energy revealed a dependency on the EFP's distance from the target, with the most significant effects observed within a range of one liner diameter. Beyond the distance of two diameters, further changes in effectiveness are minimal, with slight variations attributed to computational method inaccuracies.

Keywords: explosively formed penetrator, EFP, perforation, computational mechanics, finite element method, arbitrary Lagrangian–Eulerian

[1]PhD., Eng., Military University of Technology, Faculty of Mechanical Engineering, Gen. Sylwestra Kaliskiego St. 2, 00-908 Warsaw, Poland, sebastian.stanislawek@wat.edu.pl, ORCID: 0000-0002-6895-8413
[2]PhD., Eng., Military University of Technology, Faculty of Mechanical Engineering, Gen. Sylwestra Kaliskiego St. 2, 00-908 Warsaw, Poland, grzegorz.slawinski@wat.edu.pl, ORCID: 0000-0003-0411-0955
[3]PhD., Eng., Military University of Technology, Faculty of Mechanical Engineering, Gen. Sylwestra Kaliskiego St. 2, 00-908 Warsaw, Poland, andrzej.morka@wat.edu.pl, ORCID: 0000-0001-8645-4609

1. Introduction

The application of Explosively Formed Projectiles (EFPs) was first described in 1930s [1]. A significant increase in the number of publications in this field occurred when numerical simulation also emerged. Currently, the subject is the focus of many experimental and numerical studies. Since modelling of a EFP formation, where extreme strain rates are present among other things, is a very complex issue, numerous papers have analyze various simulation aspects. Contact interfaces, the type and mesh structure, discretization issues, detonation wave characteristics, constitutive models, and the application of alternative computational methods are disputed [2–6]. However, the majority of the research focuses on the influence of charge geometry (especially the liner shape) and other factors on projectile formation and its further performance [7–9]. Some of these studies mainly discuss the impact and penetration process and focus on the material and structure of single and multi-layered targets [10]. The process is also examined on the basis of metallographic examination of the material within the shock influence area [11, 12]. Multi point initiation may enhance EFP perforation ability because it influences projectile velocity, length- diameter ratio, and most importantly change in velocity gradient [13, 14]. As well as modelling, experimental research is also a demanding task. Radiography is utilized to observe the formation process [15]. Finally, it is important to mention that EFP formation may occur completely differently if the process occurs in water [16].

Usually a shape charge is a device in which an explosive load is used to collapse a liner, thereby creating a high energy impactor that is capable of penetrating deep into any material including high strength armor steel. EFP is considered to be a structure which has high penetration ability at long distances. In the literature, the penetration capabilities of EFPs at short distances between the charge placement and impact point are rarely considered [17]. According to the results of both simulations and experimental observations, the time required for complete projectile formation ranges from 90 to 300 µs [3, 8, 18]. However, some penetration ability already exists in an earlier project formation stage. Such a weapon can be used to perforate obstacles where the warhead is mounted directly on the target. Classic applications of EFPs include anti- tank guided missiles, anti-hull mines, and anti-helicopter munitions. The design of the light charge, which allows it to be placed close to the target, is aimed at military units that need to transport weapons in a backpack and use them for a quick penetration of structures that cannot be damaged by less invasive methods. Therefore, the aim of this study is to analyze the influence of the charge placement distance on the perforation capability for selected EFP charge configurations.

2. Investigation plan

The general EFP used at short distances should fulfil the purpose of light weight design and high penetrability. However, it is not necessary to obtain a stable shape during flight for longer distances. The casing should have appropriate dimensions to allow the liner to form a projectile and to contain a sufficient amount of explosive. Basing it on [19] a thick steel-cased charge can provide more impulse to the liner in the EFP's forming process, although it is not critical

to perforation effectiveness. Therefore, it was decided that the casing could be manufactured using the FDM (Fused Deposition Modelling) 3D printing technique and may be neglected during numerical analysis due to material low mechanical strength [20]. Furthermore, such a design makes the EFP lighter, which is important when it is carried by soldiers in their personal equipment. The prototype is presented in Fig. 1. The casing is a modular design which allows the required distance from the target to be provided.

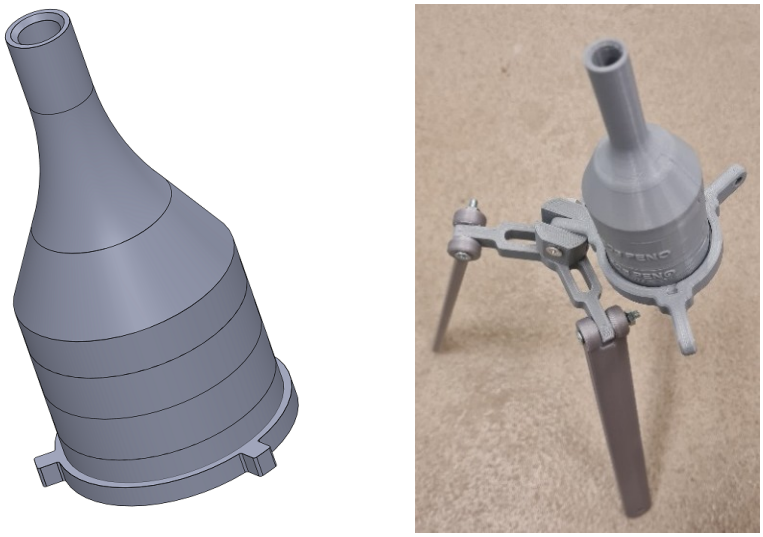

(a) (b)

Fig. 1. The concept of the EFP casing and 3D (a) printed prototype (b)

In the paper, a number of variants were analyzed. The basic concept of the design is based on [21], where experimental validation of an explosively formed projectile with variable thickness liner was presented. The authors also provided a detailed description of a numerical model including data for material models. Three designs were investigated; however, liner number II is believed to form potentially the best projectile in terms of its penetrability.

The diameter of the copper liner mentioned above was 72 mm, so it is denoted by 72c in the current paper. This variant was further used for validation purposes, which are described later. The shaped charges on the market today range from about 20 to 200 mm in diameter. Scaling the discussed case, an EFP with liner diameters of 200 mm was also modelled. In contrary to the validated model, the variants analyzed did not include a casing. The liner material was an-other issue studied with respect to penetration ability. Tantalum, copper, iron, molybdenum, and tantalum-tungsten alloys were used in EFP applications [10]. In this paper, only the most common copper and high ductility iron was investigated. The distance to the target was defined as liner diameter multiplicity. The following Table 1 gives a summary of all the variants investigated.

Table 1. EFP structure configuration studied

Symbol	Description	Liner material
72cV	72 mm liner (numerical model validation)	Copper
72c	72 mm liner (without casing)	Copper
72cM	Modified 72 liner (without casing): 75% original thickness	Copper
72i	72 mm liner (without casing)	Iron
200c	200 mm liner (without casing)	Copper

The simulation, the concept of which is depicted in Fig. 2, focused on the issue of the interaction of detonation products with the liner and penetration phenomena. The analysis concerned changes in the geometry of the projectile and its kinetic energy. For selected distances, including those at which the projectile did not achieve its final, stable properties, additional simulations were performed. For this reason, the impact distance, expressed in projectile diameters, were 0.5×D, 1×D, 2×D, 3×D (where D denotes the diameter of the liner). Initial calculations proved that further distances did not influence the result.

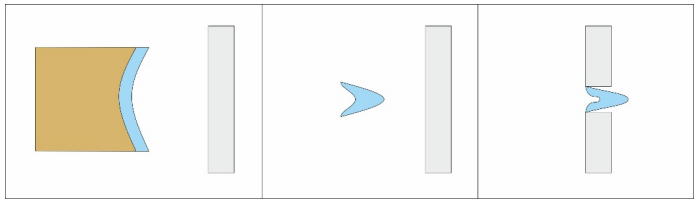

Fig. 2. The concept of the EFP casing and 3D printed prototype

3. Fundamentals of the numerical methods

The EFP formation process results in a volumetric expansion of the product of detonation and extensive plastic flow of the metal liner. Both can be successfully calculated using an Arbitrary Lagrangian–Eulerian (ALE) algorithm involving the finite element method. In the utilized method, the topology of the mesh is fixed in space, in fact leading to an Euler approach. Continuum mechanics is founded on the fundamental rules of conservation of mass, energy and momentum. A single ALE step requires performing a Lagrangian step in which a momentum equation is solved in the following form, also known as an equation of motion:

$$\sigma_{ij,j} + \rho f_i = \rho \ddot{x}_i \tag{3.1}$$

where σ is the Cauchy stress, ρ is the current density, f is the body force density and $\ddot{x}$ is acceleration. Together with the following energy equation:

$$\dot{E} = V s_{ij} \dot{\varepsilon}_{ij} - p\dot{V} \tag{3.2}$$

where E is internal energy, V is relative volume change, s is deviatoric stress tensor, ε is strain tensor and p pressure (for solids meaning normal stress).

Instead, the mass conservation equation has a simple algebraic form. In this stage, the weak formulation (Galerkin approach) is applied, which leads to the integral form of the problem equations. The stability of the calculation is satisfied by the Courant-Friedrichs Lewy (CFL) Criteria, which are based on the concept that time for elastic stress to be traversed through the element should not exceed:

$$\Delta t = 0.9\frac{L}{c} \tag{3.3}$$

where L is characteristic element length and c is speed of sound in the material:

$$c = \sqrt{\frac{E}{\rho(1-\upsilon^2)}} \tag{3.4}$$

In the advection step, all the nodes are moved to the original locations. With the updated node positions, the next step entails calculating the transport of element-centered variables. Finally, the procedure concludes with the calculation of momentum transport and subsequent updating of velocity based on the changes in node positions and variable transports. The concept for performing the advection (remap) step is taken from the CFD community, and the mass conservation equation is:

$$\frac{\partial \phi}{\partial t} + a(x)\frac{\partial \phi}{\partial x} = 0 \tag{3.5}$$

where a is the flux velocity and ϕ symbolizes the conserved quantities.

A Van Leer second order monotone upwind scheme for conservation laws (MUSCL) [22] was applied to solve the advection step with the half index shift (HIS) improvement proposed by [23].

The material motion during the step should be less than the characteristic length of the studied element Δx, which means that the Courant number should be less than one:

$$C = \frac{u\Delta t}{\Delta x} < 1 \tag{3.6}$$

where $u\Delta t$ is the transporting distance between adjacent elements.

The problem was solved using axial symmetry, and it was ensured that disturbances related to the limited size of the Euler domain did not affect the course of the phenomena occurring. This goal was achieved through the appropriate implementation of initial and boundary conditions.

4. Fundamentals of the numerical methods

4.1. Geometry and boundary conditions

The basic model (72cV) represents the warhead described in [21]. The geometric configuration of the EFP is illustrated in Figure 3, where the warhead length and liner diameter were both 72 mm, with a casing thickness of 5 mm. The liner was an axisymmetric spherical shell structure, and its thickness is 4 mm. The steel plate, which serves as the tar-get, had a thickness of 10 mm, making it penetrable for every scenario considered.

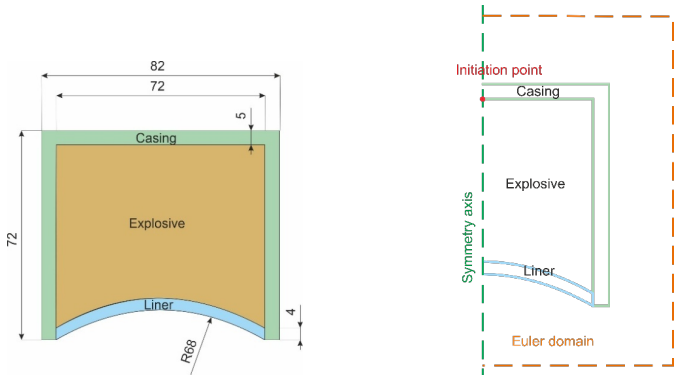

(a) (b)

Fig. 3. EFP basic variant (72cV) geometry (a) and model concept (b)

The 72cV computational model contains the EFP (liner, casing, explosive), air, and a target plate. The arbitrary Lagrangian–Eulerian (ALE) algorithm implemented in the LS-DYNA environment [24], a widely used tool for blast modelling, was chosen to provide the numerical solution to the problem. The basic mesh density is 0.2 mm, which allows us to have 15 elements per liner thickness and is also appropriate according to [25–27]. The explosive was initiated at the centre point of the back of EFP, and the one-point initiation method was adopted. An axially symmetric model was used.

The numerical models of the variant (72c-200i) further discussed utilize the above assumptions with some modifications. Preliminary analyses showed that air is not an important factor, and was not modelled for simplification. The casing was also not modelled, since in the designed warhead it was made of low strength material. The models differed in size and their geometry were built by scaling the 72c variant.

4.2. Material modelling

The EFP liner was made of copper or Armco iron respectively. The casing was 45 steel grade, the target was ARMOX 500T steel and 8701 explosive was used as the charge. Material modelling is one of the key factors which influences the projectile formation and perforation process. The casing was described by a plastic kinematic mate-rial model. The liner and target plate required a more advanced approach due to extreme deformations. Therefore, the Johnson–Cook model was used, where effective plastic stress is defined as a function of the strain, strain-rate, and the temperature. The Gruneisen equation of state is used in conjunction with the constitutive model. The simplified detonation model based on [28] was applied and the products of detonation were modelled by the Jones–Wilkins–Lee (JWL) equation of state, that is the pressure as a function of density and internal energy. The theoretical foundations of these mathematical material models are discussed widely in the literature [24], and therefore will be not provided in the content of this paper. Materials data is taken exactly from the previously mentioned paper [24] with the only difference that the target plate is simulated using the Johnson–Cook model according to [29].

4.3. Model validation

The paper [21] was used in terms of the EFP formation process as the basis for validation of the basic 72cV numerical model proposed in this paper. Than other models were elaborated assuming that they can predict properly physical phenomena because were derived based on prior validated model. This means that other models were indirectly verified; however, the main purpose of this work was not to design a projectile able to perforate a particular target but to study the close distance penetration capabilities. As stated in [21], all tested EFP were completely formed at 120 µs. The validation was based on comparing the dimensions of the projectile and its velocity. The results presented in Table 2 show a maximum error of 6%, which is fully satisfactory.

Table 2. Validation results comparison

	Length (mm)	**Diameter (mm)**
Type II liner [21]	52.0	33.1
72cV	50.4	31.2
Error [%]	3	6

5. Results and discussion

5.1. Projectile formation process

The process of penetrator formation, for the selected variant 72c, is shown in Fig. 4a (the shapes presented in the figure represent two-dimensional cross-sections). The near axial part of the liner moved the fastest and formed the projectile's head, but fragments further from the axis of symmetry created its tail. The application of the constitutive model with the failure option allowed for the observation of liner fragmentation due to the limited tensile strength of copper. The EFP should contain practically the entire mass of the liner, and here the described loss was insignificant. Beyond 120 µs changes in the geometry were not substantial (final diameter and length were 35.9 and 44.5 respectively), this refers to 180 mm distance, which can be expressed as 1.8 diameter of the liner (1.8×D). Another analysed factor was the kinetic energy of the projectile, which resulted from the interaction of the detonation wave with the liner material. This parameter continued to increase until it reached its maximum value. At this point, the expansion of detonation products no longer affected the projectile's energy. The only factor that could gradually and slowly reduce it is air resistance. However, this is considered a secondary effect and was not taken into account in any simulation. Given the presence of numerical noise, it was imperative to establish a criterion for final assessment of the maximum energy. It was defined as 99% of the value at the termination time of the simulation, and in the case discussed, it was achieved after 51 µs. Thus, it can be seen that this was before the projectile reached its final shape.

Variant 200c represents a geometrically upscaled problem in reference to 72c while maintaining the other conditions. This resulted in a longer projectile formation time (320 µs), however, the other analysed parameters remained analogous. The Fig. 4b preserves the size of the picture consequently it looks similar to other variants.

In 72cM, where a 3mm-thick liner was utilized, a projectile with a smaller final diameter was formed. The process was similar to the previous variant and also after 90 µs, changes in the geometry were small. Also maxi-mum energy was achieved at the same time. However, its value was equal to 25 kJ in contrast with 21.5 kJ. Summarizing, a thinner liner and lower mass results in an EFP of smaller diameter (91% 72c) and higher energy.

In the case of the 72i projectile, Armco material was used for modelling the liner, which is an alloy with a high iron content and large ductility. Fig. 1d shows a significant difference compared to a liner made of copper. Probably due to lower ductility, the final projectile had a wider diameter and a slightly higher kinetic energy of 22.6 kJ. Also in this case, after 90 µs, the shape changes were not fundamental, and the final energy level was reached after 56 microseconds.

In summary, considering all the cases studied, it can be concluded that the EFP reached its final parameters after approximately 90 µs (or 320 µs for the 200c case). During this time, the projectile travelled a distance of 134 mm (or 476 mm) which is 1.86×D. Further geometry changes would be caused by weak dynamic effects or being associated with the resistance to motion.

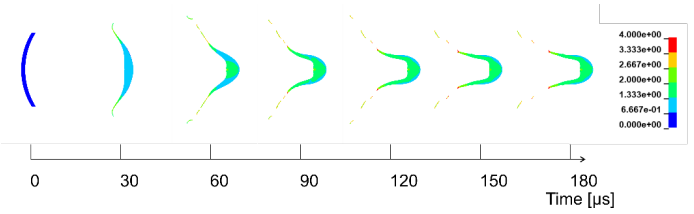

(a)

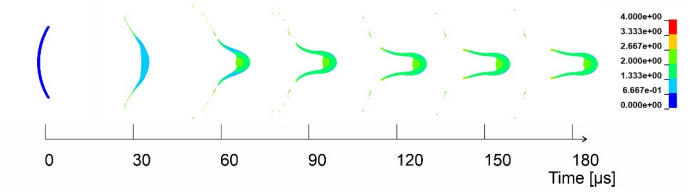

(b)

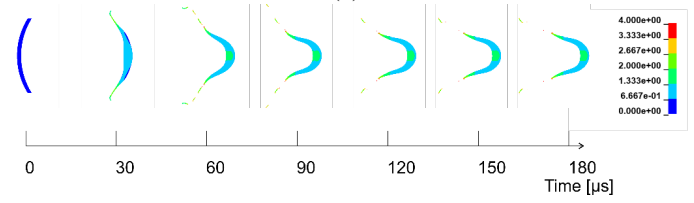

(c)

Figure continued on the next page

Figure continued from the previous page

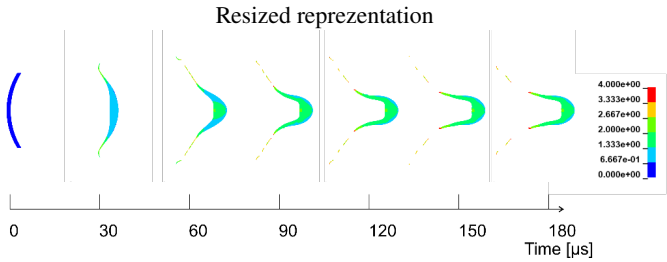

(d)

Fig. 4. Effective plastic strain distribution at different moments in time for EFP formation: a) 72c, b) 72cM, c) 72i, d) 200c

5.2. Penetration of the armor plate

The findings related to the issue of projectile formation indicated that a distance corresponding to nearly two diameters of the liner allows a target to be struck with maximum effectiveness. The ability to penetrate targets positioned closer remains an open question. In the study, it was considered that an effective way to see how closer distances affect performance is the issue in which the projectile perforates a plate of relatively insignificant thick-ness, i.e., 10 mm, and then its kinetic energy is examined. The fact that the projectile had not reached the final shape or had not been propelled to maximum speed by the detonation products had a nonlinear impact on its ability to penetrate steel material. Therefore, it was necessary to perform a special numerical study in which the perforation process is simulated.

The assumed thickness of the armour plate allowed for its perforation in each of the cases analysed. Fig. 5 presents the process of perforation of the 72c variant at the maximum distance (3×D) for selected moments in time. Significant deformation of projectile and target materials are seen, which resulted in a hole noticeably bigger than the projectile's diameter. In the final stage of the simulation, a negligible material amount of the liner underwent partial reflection, and the plastically deformed plate did not continue changing its geometry. The plugging mechanism of the perforation process is observed, which is a typical failure mode when moderately thick ductile metal plates are struck by blunt missiles.

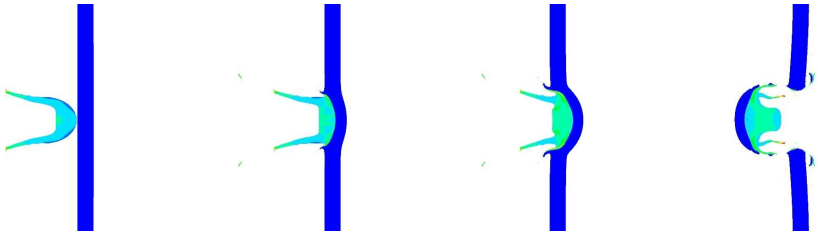

(a) (b) (c) (d)

Fig. 5. The simulation of the perforation process of EFP for 72c, where the warhead was placed at a distance of 3×D from the target: a) 280 µs, b) 290 µs, c) 300 µs, d) 320 µs

The perforation of the armour plate resulted in significant deformation of both copper and armoured steel com-ponents. This caused a rapid decrease in the velocity of the projectile and, consequently, its kinetic energy. In Fig. 6 the graphs of kinetic energy versus time are presented for different warhead locations for the single design variant 72c. During the initial 30-51 microseconds, depending on the distance, there is a rise in the liner's energy resulting from the load by detonation products, followed by a swift dissipation of energy upon collision with the plate. After the perforation process, when the main part of the projectile passes the target, there are still slight drops on the charts. This is related to the fragments of material that detached from the main part of the projectile and reached the plate later. In the final phase, the energy was not changed any more, and this value can be considered as a characteristic parameter for each case studied.

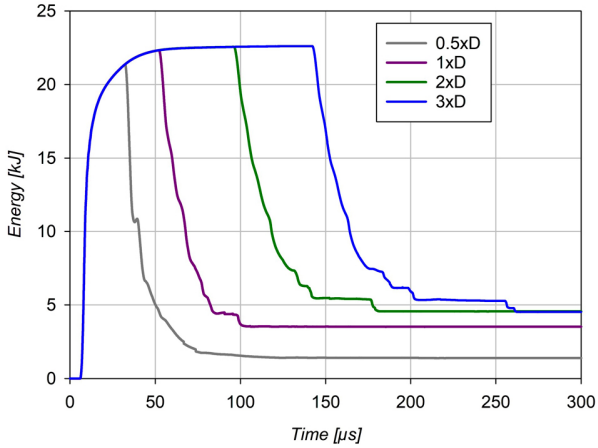

Fig. 6. Kinetic energy time history of copper liner/EFP for 72c, where the warhead was placed at different distances from the target steel plate

Based solely on a single case, it is not possible to formulate general conclusions. Therefore, an analysis of three additional cases previously described was planned, again testing various distances from the impacted target. In variant 72cM, a thinner liner was used, which, as mentioned, ensured a projectile with higher energy and greater mass concentration around its axis. Testing at distances of 2×D and beyond yielded an energy of 8.9 kJ after plate perforation. The EFP with an iron liner (72i) had a significantly lower final energy of 4.5 kJ, again for distances of 2×D and longer. The 200 mm diameter projectile (200c) had a larger mass and naturally higher kinetic energy, making it not directly comparable to the cases previously discussed. However, results are analogous in relation to its smaller counterpart. Data for all cases are compiled in Table 3, where both the numerical values of energies and their dissipations on a percentage scale were included.

Table 3. EFP kinetic energy before and after impact

Symbol	Maximum energy [kJ]	Final energy [kJ] / %			
		3×D	**2×D**	**1×D**	**0.5×D**
72c	21.5	6.2 / 29%	6.1 / 28%	4.7 / 22%	2.3 / 11%
72cM	24.8	8.9 / 36%	9.0 / 36%	6.0 / 24%	3.8 / 15%
72i	22.6	4.5 / 20%	4.6 / 20%	3.5 / 15%	1.4 / 6%
200c	461	135 / 29%	130 / 28%	103 / 22%	52.8 / 11%

6. Conclusions

The process of explosive formation of projectiles is highly sensitive to even minor inhomogeneities in the micro-structure of materials. For this reason, developing a prototype charge experimentally is difficult and quite costly. Through the utilization of computer simulation methods in this study, it was possible to analyse both the formation process of the penetrator and its penetrating capabilities. The adoption of an axisymmetric model facilitated the development of precise computational models requiring a relatively small number of finite elements, thus enhancing computational efficiency. Moreover, the core numerical model was successfully validated based in quantitative terms on the available data.

The effectiveness of an Explosively Formed Penetrator (EFP) as determined by numerical calculations is a nonlinear function of its distance from the target. Particularly at close ranges, under two diameters of the liner, the projectile fails to reach its optimal parameters, impacting the target with relatively low velocity. This effectiveness is also deteriorated by the projectile's geometry, which at this moment is still not final. Thus, impact is not concentrated in a narrow area, leading to less effective perforation. Studies on the projectile's energy post armour perforation revealed a dependency on the EFP's distance from the target, with the most significant effects observed within a range of one liner diameter. Be-yond a distance of two diameters, further changes in effectiveness are minimal, with slight variations attributed to computational method inaccuracies. This highlights the intricate interplay between distance, projectile geometry, and penetrative capability in the design and application of EFPs. The analyses conducted have demonstrated that the specific design of the EFP, where the casing is made of low-strength material and the warhead is placed at a short distance from the target, enables effective target engagement, rendering it valuable for special applications.

Acknowledgements

The article was co-financed from the state budget of Poland and awarded by the Minister of Science within the framework of the Excellent Science II Programme. The research was conducted as part of the implementation of the university research grant supported by the Military University of Technology (No. UGB 22-839/2023).

References

[1] W. Payman, D. Whitley, and H. Titman, "Explosion waves and shock waves, Part II - The shock waves and explosion products sent out by blasting detonators", *Proceedings of the Royal Society of London. Series A*, vol. 148, no. 865, pp. 604–622, 1935.

[2] W.H. Lee, *Computer Simulation of Shaped Charge Problems*. California, USA: World Scientific Publishing Co Inc, 2006.

[3] R.G. Johnson and R.A. Stryk, "Some considerations for 3D EFP computations", *International Journal of Impact Engineering*, vol. 32, no. 10, pp. 1621–1634, 2006, doi: 10.1016/j.ijimpeng.2005.01.011.

[4] E.A. Taylor, "Simulation of hollow shaped charge jet impacts onto aluminium whipple bumpers at 11 km/s", *International Journal of Impact Engineering*, vol. 26, no. 1–10, pp. 773–784, 2001, doi: 10.1016/S0734-743X(01)00129-4.

[5] U. Nyström and K. Gylltoft, "Numerical studies of the combined effects of blast and fragment loading", *International Journal of Impact Engineering*, vol. 36, no. 8, pp. 995–1005, 2009, doi: 10.1016/j.ijimpeng.2009.02.008.

[6] J.F. Molinari, "Finite element simulation of shaped charges", *Finite Elements in Analysis and Design*, vol. 38, no. 10, pp. 921–936, 2002, doi: 10.1016/S0168-874X(02)00085-9.

[7] F. Hu, H. Wu, Q. Fang, J.C. Liu, B. Liang, and X.Z. Kong, "Impact performance of explosively formed projectile (EFP) into concrete targets", *International Journal of Impact Engineering*, vol. 109, pp. 150–166, 2017, doi: 10.1016/j.ijimpeng.2017.06.010.

[8] J. Wu, J. Liu, and Y. Du, "Experimental and numerical study on the flight and penetration properties of explosively-formed projectile", *International Journal of Impact Engineering*, vol. 34, no. 7, pp. 1147-1162, 2007, doi: 10.1016/j.ijimpeng.2006.06.007.

[9] J. Liu, Y. Long, C. Ji, M. Zhong, and Q. Liu, "The influence of liner material on the dynamic response of the finite steel target subjected to high velocity impact by explosively formed projectile", *International Journal of Impact Engineering*, vol. 109, pp. 264–275, 2017, doi: 10.1016/j.ijimpeng.2017.07.002.

[10] J. Liu, Y. Long, C. Ji, Q. Liu, M. Zhong, and Y. Zhou, "Influence of layer number and air gap on the ballistic performance of multi-layered targets subjected to high velocity impact by copper EFP", *International Journal of Impact Engineering,* vol. 112, pp. 52–65, 2018, doi: 10.1016/j.ijimpeng.2017.10.001.

[11] A. Kurzawa, D. Pyka, M. Bocian, K. Jamroziak, and J. Śliwiński, „Metallographic analysis of piercing armor plate by explosively formed projectiles", *Archives of Civil and Mechanical Engineering*, vol. 18, no. 4, pp. 1686–1697, 2018, doi: 10.1016/j.acme.2018.06.006.

[12] H. Fu, J. Jiang, J. Men, and X. Gu, "Microstructure Evolution and Deformation Mechanism of Tantalum-Tungsten Alloy Liner under Ultra-High Strain Rate by Explosive Detonation", *Materials,* vol. 15, no. 15, art. no. 5252, doi: 10.3390/ma15155252.

[13] W. Li, X. Wang, and W. Li, "The effect of annular multi- point initiation on the formation and penetration of an explosively formed penetrator", *International Journal of Impact Engineering*, vol. 37, no. 4, pp. 414–424, 2010, doi: 10.1016/j.ijimpeng.2009.08.008.

[14] G. Ma, G. He, Z. Qiao, and Y. Zhang, "Study on the Influence of Initiation Model on the Forming Characteristics of MEFP Warhead", *Shock and Vibration*, vol. 2021, art. no. 5563622, 2021, doi: 10.1155/2021/5563622.

[15] J. Borkowski, Z. Wilk, P. Koślik, L. Szymańczyk, and B. Zygmunt, „Application of sintered liners for explosively formed projectile charges", *International Journal of Impact Engineering*, vol. 118, pp. 91–97, 2018, doi: 10.1016/j.ijimpeng.2018.04.009.

[16] Z. Zhang, H. Li, L. Wang, G. Zhang, and Z. Zong, "Formation of Shaped Charge Projectile in Air and Water", *Materials*, vol. 15, no. 21, art. no. 7848, 2022, doi: 10.3390/ma15217848.

[17] P. Malesa, G. Sławiński, and K. Pęcherzewska, „Numerical Analysis and Experimental Test for the Development of a Small Shaped Charge", *Applied Sciences*, vol. 11, no. 6, art. no. 2578, 2021, doi: 10.3390/app11062578.

[18] R. Li, W.B. Li, X.M. Wang, and W.B. Li, „Effects of control parameters of three-point initiation on the formation of an explosively formed projectile with fins", *Shock Waves*, vol. 28, no. 2, pp. 191–204, 2018, doi: 10.1007/s00193-017-0725-9.

[19] L. Ding, J. Jiang, J. Men, and S. Wang, "Modeling and Simulation of the Effects of Steel Casing Confinements on Formation of Explosively Formed Projectile", *Journal of Physics: Conference Series*, vol. 1624, 2020, doi: 10.1088/1742-6596/1624/2/022008.

[20] A. Al Sabouni-Zawadzka, W. Gilewski, and A. Zawadzki, „Experimental investigations on mechanical properties of 3D-printed tensegrity-inspired metamaterials based on 4-strut simplex module", *Archives Of Civil Engineering,* vol. 70, no. 3, pp. 343–357, 2024, doi: 10.24425/ace.2024.150987.

[21] D. Yang and J. Lin, "Numerical Investigation on the Formation and Penetration Behavior of Explosively Formed Projectile (EFP) with Variable Thickness Liner", *Symmetry*, vol. 13, no. 8, art. no. 1342, 2021, doi: 10.3390/sym13081342.

[22] B. Van Leer, "Towards the Ultimate Conservative Difference Scheme. IV. A New Approach to Numerical Convection", *Journal of Computational Physics*, vol. 23, no. 3, pp. 276–299, 1977, doi: 10.1016/0021-9991(77)90095-X.

[23] D.J. Benson, "Vectorizing the Right-Hand Side Assembly in an Explicit Element Program", *Computer Methods in Applied Mechanics and Engineering*, vol. 73, no. 2, pp. 147–152, 1989, doi: 10.1016/0045-7825(89)90109-6.

[24] J. Hallquist, *LS-Dyna Theory Manual*. Livermore, CA, USA: LSTC, 2006.

[25] J.J. Munoz, "On the modeling of incompressibility in linear and non-linear elasticity with the master-slave approach", *International Journal for Numerical Methods in Engineering*, vol. 74, no. 2, pp. 269–293, 2008, doi: 10.1002/nme.2166.

[26] H.O. Agu, A. Hameed, and G.J. Appleby-Thomas, "Application of Shell Jetting Analysis to Determine the Location of the Virtual Origin in Shaped Charges", *International Journal of Impact Engineering*, vol. 122, pp. 175–181, 2018, doi: 10.1016/j.ijimpeng.2018.04.014.

[27] D. Pyka, et al., „Numerical and Experimental Studies of the ŁK Type Shaped Charge", vol. 10, no. 19, art. no. 6742, 2020, doi: 10.3390/app10196742.

[28] E.D. Giroux, *HEMP User's Manual*. Livermore, CA, USA: Lawrence Livermore National Lab. (LLNL), 1973.

[29] M. Klasztorny, M. Świerczewski, P. Dziewulski, and A. Morka, „Numerical Modelling and Design of ALFC Shield Loaded by 20 mm FSP Fragment", *Journal of KONES*, vol. 19, no. 4, pp. 301–313, 2015, doi: 10.5604/12314005.1138465.

Analiza zdolności perforacyjnych pocisków formowanych wybuchowo stosowanych w bliskim dystansie

Słowa kluczowe: penetratory formowane wybuchowo, EFP, perforacja, mechanika komputerowa, metoda elementów skończonych, sprzężona analiza Eulera–Lagrange'a

Streszczenie:

Artykuł przedstawia badanie zdolności perforacyjnych penetratorów formowanych wybuchowo (EFP) stosowanych na krótkich dystansach. Analizowano projekt głowicy bojowej z obudową wykonaną z materiału o niskiej wytrzymałości, którą można montować bezpośrednio na przeszkodzie. Takie rozwiązanie sprawia, że głowica jest szczególnie przydatna w sytuacjach wymagających szybkiej perforacji wytrzymałych konstrukcji. Zagadnienie rozwiązano przy użyciu metod modelowania i symulacji, wdrożonych w oprogramowaniu LS-Dyna, które stanowi rozbudowaną implementację metody elementów skończonych z jawnym całkowaniem równań ruchu, dedykowaną dla zagadnień dynamicznych. W celu poprawy efektywności obliczeń założono osiową symetrię problemu, gdzie dyskretyzacja przestrzeni została wykonana przy użyciu elementów dwuwymiarowych. Bazowy model numeryczny został pomyślnie zwalidowany, na podstawie dostępnych danych eksperymentalnych, w sposób ilościowy. Analiza wykazała, że skuteczność EFP określona na podstawie obliczeń numerycznych, jest nieliniową funkcją jego odległości od celu. Na małych dystansach, tj. poniżej dwóch średnic wkładki, pocisk nie osiąga swoich optymalnych parametrów, uderzając w cel z relatywnie niską prędkością. Skuteczność jest również pogarszana przez geometrię pocisku, która w tym momencie wciąż nie jest ostateczna. W związku z tym, energia oddziaływania uformowanego pocisku nie jest skoncentrowana na małej powierzchni, co prowadzi

do mniej efektywnej perforacji. Badania energii pocisku po przebiciu celu ujawniły silną zależność od odległości EFP, przy czym najbardziej znaczący wpływ zaobserwowano dla jednej średnicy wkładki. Po przekroczeniu odległości dwóch średnic dalsze zmiany są nieznaczne, a niewielkie różnice przypisane są niedokładności metody obliczeniowej. Podsumowując zastosowanie EFP do rażenia celów w bliskim dystansie jest efektywne, jeżeli zapewniona zostanie wymagana, nieznaczna odległość od przeszkody. Skuteczna aplikacja ładunku może być zrealizowana poprzez wykonanie obudowy z materiału o małej gęstości, nie powodując znacznego wzrostu masy całkowitej. Rezultaty tej pracy mogą być wykorzystane w przyszłości do zaprojektowania ładunków będących na wyposażeniu sił specjalnych.

Received: 2025-02-25, Rervised: 025-05-06